Recent Developments in the F-16 Flutter Suppression with Active Control Program

R P Peloubet Jr ,* R L Haller,† and R M Bolding‡
General Dynamics, Fort Worth, Texas

A series of wind tunnel tests of the F 16 flutter model employing active control to suppress flutter was con ducted during October 1981 These tests complemented the initial series of tests conducted in February 1979 Questions associated with the validity of the measured open loop frequency response function (FRF) as a true indicator of the model's unaugmented stability with the flutter suppression system (FSS) engaged were resolved by temporarily disengaging the system The accuracy of the measured open loop FRF as a function of excitation level, frequency resolution and number of ensemble averages was investigated. FSS gain and phase margins were measured directly Tests were conducted for a simulated actuator failure Flutter suppression was demonstrated for two external store configurations One configuration exhibited symmetric flutter and the other exhibited antisymmetric flutter

Nomenclature

G_i	= FSS sensor gain
G_Σ	= FSS ensemble gain
M	= Mach number
q	= dynamic pressure
s	= Laplace variable
T	= closed loop frequency response function measured at terminating point (δ_I/δ_E)
Δf	= frequency increment
δ_A	= actual control surface deflection
δ_C	= commanded control surface deflection
δ_E	= excited control surface deflection
δ_I	= feedback FSS control surface deflection in the loop
δ_O	= feedback FSS control surface deflection out of the loop
δ_1 δ_4	= signal of points 1 and 4 respectively
τ	= time constant
ϕ_i	= FSS sensor phase shift
ω_r	= reference frequency

Introduction

THE objectives of the F-16 flutter suppression program are 1) to develop the technology and 2) to increase the credibility of using active controls to suppress wing/store flutter on a flight test demonstration aircraft and/or operational aircraft The status of this program through the February 1979 F 16 flutter suppression wind tunnel tests has been published.[1 3] The present paper presents the results of more recent wind tunnel tests which were conducted in Oc tober 1981 under the sponsorship of AFWAL with the cooperation of NASA Langley Research Center More detailed discussions of these activities are presented in Refs 4 and 5 Recent related efforts by other researchers in active flutter suppression are described in Refs 6 9

Received April 8, 1983; presented as Paper 83 0995 at the AIAA/ASME/ASCE/AHS 24th Structures Structural Dynamics and Materials Conference, Lake Tahoe Nev May 2 4 1983; revision received March 19 1984

*Engineering Chief Associate Fellow AIAA
†Senior Engineering Specialist
‡Engineering Specialist Member AIAA

During the February 1979 tests one external store con figuration, identified as Configuration 33, was tested to a dynamic pressure with the flutter suppression system (FSS) engaged that was 100% above the dynamic pressure at which flutter occurred without the FSS engaged Post wind tunnel test data reduction results caused some uncertainty about whether the model was in the flutter region over the entire wind tunnel path while the FSS was engaged This uncertainty was produced by a corresponding uncertainty in the accuracy of the open loop frequency response function (FRF) when measured with the loop physically closed Hence, one of the objectives of the October 1981 wind tunnel tests was to retest Configuration 33 and determine its flutter region in an explicit manner Other objectives were to determine the accuracy of the measured open loop FRF and investigate means of im proving it to determine whether flutter could be suppressed with one flaperon surface while the actuator of the other flaperon was locked in a neutral position simulating an ac tuator failure and to test a store configuration that produced symmetric flutter to confirm that the flaperons could be used to suppress symmetric as well as antisymmetric flutter

F-16 FSS Model and Systems

The F 16 flutter model, shown in Fig 1, is a full span, quarter scale model designed to fly on a cable system in the NASA LaRC Transonic Dynamics Tunnel (TDT) The original use of the model was to investigate wing/store flutter characteristics Subsequently, it was modified to incorporate a FSS and was wind tunnel tested in February 1979 under the sponsorship of General Dynamics The modifications made to the model included the addition of miniature hydraulic ac tuators to activate the flaperons and the installation of a hydraulic system in its fuselage Electrical power to the motor driving the hydraulic pump in the fuselage was supplied through the umbilical cord from an external source

A Control Law Implementation Package (CLIP) was developed for implementing the FSS control laws Electrical signals from accelerometer sensors on the model were sent through the umbilical cord to the CLIP located in the control room and then returned after processing, through the um bilical cord to the servoactuators A block diagram of the CLIP is shown in Fig 2 From one to three sensor signals can be used on the control law Each signal is obtained as the sum of symmetrically located sensors on the left and right wings for symmetric flutter or the difference for antisymmetric flutter.

Each signal is passed through a high pass filter of the form $s/(s+20)$ Each signal can be operated upon to obtain a desired gain and phase angle at a selected reference frequency The operation between points 1 and 4 on Fig. 2 is illustrated by Eq (1)

$$\delta_4 = G_1\left[\frac{\cos\phi_1}{\omega_r} - \frac{\sin\phi_1}{1+s}\right]\delta_1 \simeq \left[\frac{G_1}{\omega_r}\angle\phi_1\right]\delta_1 \text{ at } \omega=\omega_r \quad (1)$$

The signals are then summed and the combined signal is optionally amplified by a variable gain, a variable all-pass filter, and a variable low pass filter The output signal is fed back to the servoactuator if the loop is closed, or is used only for monitoring if the loop is open Each of the numbered points on Fig 2 can be monitored

Four feedback circuits identical to the one shown in Fig. 3 are employed Both the symmetric and antisymmetric FSS employed two feedback circuits, one in the loop and one out of the loop While one loop is closed, the other loop can be used to investigate other sensor/control law combinations The two loops can be interchanged by a switching system To disengage the FSS the gain of the in the loop circuit is set to zero To measure the open loop FRF with the loop physically open (below the flutter speed) the control law of interest is set up in the out-of-the-loop circuit with zero gain on the in the loop circuit A random excitation signal is applied and the ratio of δ_O to δ_E is measured by means of a real time frequency analyzer Above the flutter speed, the FSS was implemented with the in the loop circuit and could not be physically opened For that use, the open loop FRF was measured by two methods which are referred to here as the direct and indirect methods The direct method obtains the open loop FRF as the ratio of the feedback signal to the command signal (error signal)

$$\text{Open-loop FRF} = \delta_I/\delta_C \quad (2)$$

The indirect method first obtains the closed loop FRF as the ratio of the feedback signal to the excitation signal as in dicated by

$$T = \delta_I/\delta_E \quad (3)$$

and then obtains the open-loop FRF by the algebraic manipulation of this FRF as indicated by

$$\text{Open loop FRF} = T/(1-T) \quad (4)$$

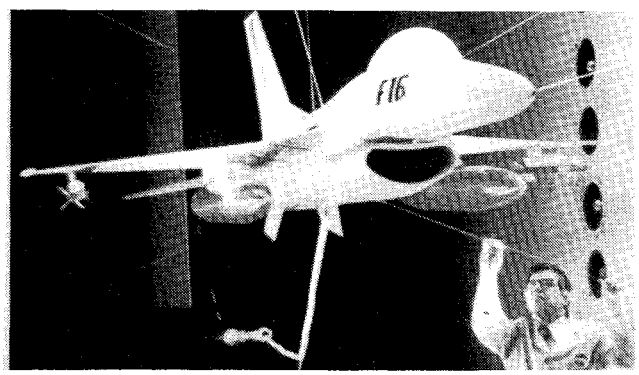

Fig 1 One quarter scale F 16 flutter suppression model

Configuration 33

Store Configuration 33 is shown in Fig 4 It has a three-bay 370 gallon fuel tank with the center bay empty on the inboard station, a GBU 8 weapon on the next outboard station, and an AIM 9 missile on the tip The locations of the six ac celerometers mounted on each wing are shown

1979 Wind Tunnel Tests

A flutter condition without the FSS engaged was obtained at the condition indicated by the solid circle in Fig. 5 The flutter mode is antisymmetric at a frequency of 8 6 Hz The wind tunnel conditions were then reduced to the condition indicated by the triangular symbol where the open-loop FRF was measured for a control law which used sensor 5 Subsequently the FSS was engaged The model then was tested along the path marked by the hexagonal symbols At the three conditions indicated by 1, 2, and 3 the open-loop FRF was measured on-line by the direct method The Nyquist plot showed a counterclockwise (CCW) loop at 8 6 Hz that barely enclosed the $(-1,0)$ point Wind tunnel data recorded on magnetic tape were used during post wind tunnel test data reduction to obtain the open loop FRF at the same three conditions via the indirect method [3] The Nyquist plot of the open loop FRF confirmed that the loop associated with the 8 6 Hz flutter mode was CCW and encircled the $(-1,0)$ point for conditions 1 and 3 but indicated the loop to be clockwise (CW) for condition 2 Hence, the indirect method indicated that the model with the FSS engaged was operating in the flutter region at conditions 1 and 3, but out of the flutter region at condition 2 Open loop FRF data were not measured at conditions indicated by the other hexagonal symbols Wind tunnel noise makes it virtually impossible to measure the open loop FRF with the loop closed near the flutter boundary and flutter frequency [1,2] However, the flutter boundary shown in Fig 5 would indicate condition points 1, 2, and 3 were deep in the flutter region and good measurements should be expected One of the objectives of the October 1981 wind tunnel tests was to resolve this uncertainty

1981 Wind Tunnel Tests

Prior to conducting the October 1981 wind tunnel tests, ground tests of the model were conducted to measure vibration modes and frequencies and open-loop FRF relating wing mounted accelerometer responses to the control surface actuator input signal The mathematical model of the flutter model was tuned to improve its correlation with the measured data The tuned model then was used to develop a FSS using sensor 3 that appeared to be better than the FSS employed during the 1979 wind tunnel tests Referring to Fig 2, the control law can be defined by Eq (5) This control law was identified as CL100

$$\begin{array}{llll} s/(s+20) & = \text{engaged} & G_2 & = G_3 = 0 \\ \omega_r & = 50 \text{ rad/s} & G_\Sigma & = 4\,0 \\ G_1 & = 1\,35 & \tau_1 & = 0 \\ \phi_1 & = -14 \text{ deg} & \tau_2 & = 0 \end{array} \quad (5)$$

During the initial run of the October 1981 tests the model was tested along a path very close to the path in Fig 5 in dicated by the hexagons marked 1, 2, and 3 The flutter

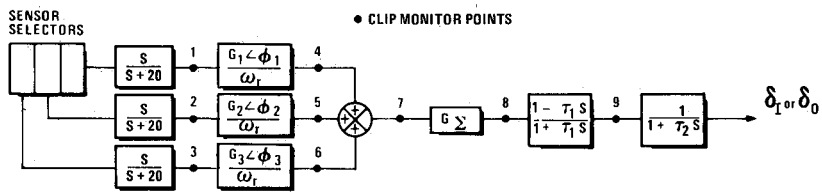

Fig 2 Control law implementation package

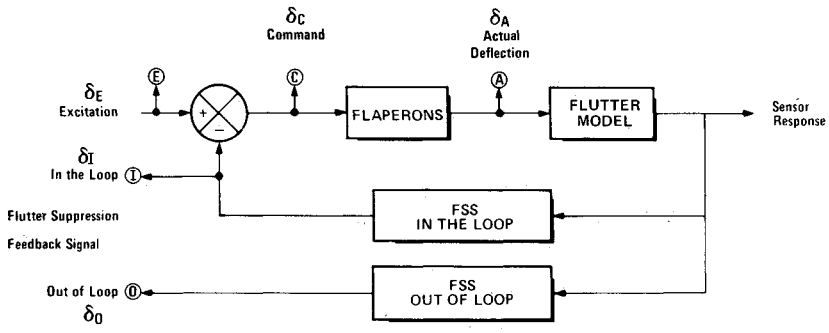

Fig 3 Wind tunnel test configuration of model flutter suppression system

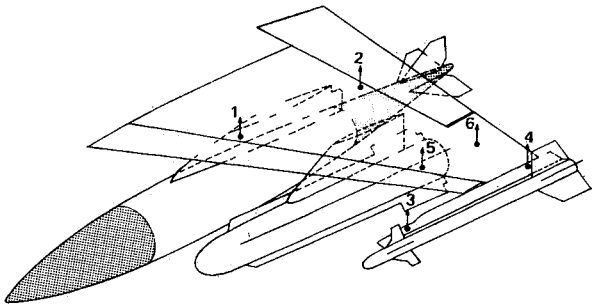

Fig 4 F 16 wing/store Configuration 33

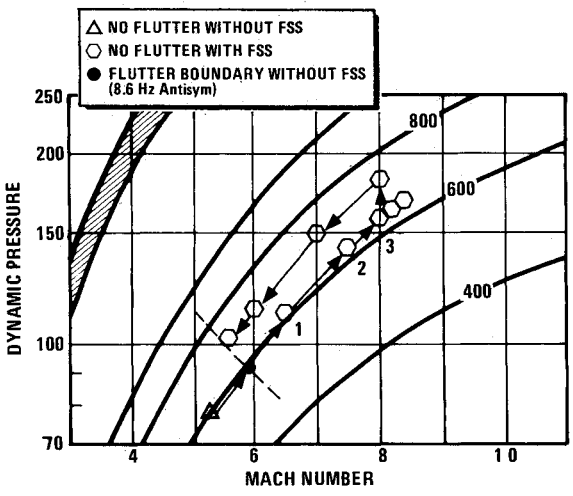

Fig 5 1979 test conditions for Configuration 33

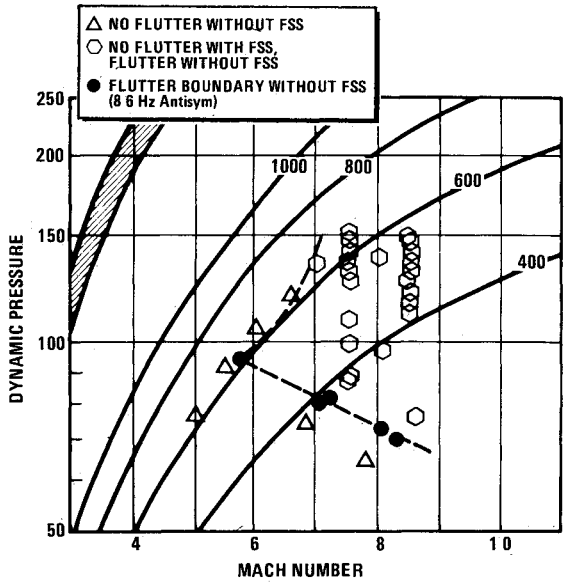

Fig 6 Flutter boundary for Configuration 33 defined by 1979 and 1981 test data

condition without the FSS engaged was the same With the FSS engaged, the path up the lower curve in Fig 5 was ter minated at Mach number 0 66 The dynamic pressure was increased, while the Mach number was held constant until a condition slightly above the upper path in Fig 5 (indicated as a descending path through the hexagon symbols) was reached At that condition (approximately 140 psf) the open loop FRF was measured by the direct method The measurement in- dicated that the model was no longer in the flutter region At that condition the FSS was disengaged and the model was indeed stable As the dynamic pressure and Mach number were reduced along a path slightly above the upper path in Fig 5, without the FSS engaged, the model was stable (outside the flutter region)

Subsequently, the model was tested along several wind tunnel paths to determine the flutter region A composite plot representing data obtained during these runs is shown in Fig 6 The solid circular symbols indicate flutter conditions that were obtained without the FSS engaged The open hexagonal symbols indicate conditions that were confirmed to be in the flutter region by disengaging the FSS long enough to see the flutter mode develop and then re engaging the FSS Con ditions indicated by the hexagonal symbols were explicitly identified as inside the flutter region Conditions indicated by the triangular symbols were identified as being outside the flutter region The upper and lower boundaries of the flutter region are indicated by the dashed lines By comparing Fig 5 with Fig 6 it can be seen that the lower path followed during the February 1979 tests was very close to the upper boundary of the flutter region Hence, it was difficult to obtain accurate open-loop FRF measurements with the loop closed and there was uncertainty about whether the model was in the flutter region If the dynamic pressure of the lower flutter boundary at Mach number 0 85 is compared to the maximum dynamic pressure with the FSS engaged at Mach number 0 85, it is clear that an increase of over 100% in dynamic pressure was achieved However, for the path that was tested in 1979 it is also clear that a comparison of the flutter boundary dynamic pressure with the maximum dynamic pressure obtained with FSS is not as meaningful

All of the testing inside the flutter region shown in Fig 6 was accomplished using the control law that was developed analytically and defined by Eq (5) with the exception that the G_Σ gain was increased by a factor of 2 The gain was increased because the initial open loop FRF measurement that was made slightly above the flutter boundary indicated that the gain could be safely increased by a factor of 2 without in creasing the lower crossover point on the CCW loop above 0 5 on the negative axis This control law was identified as CL103

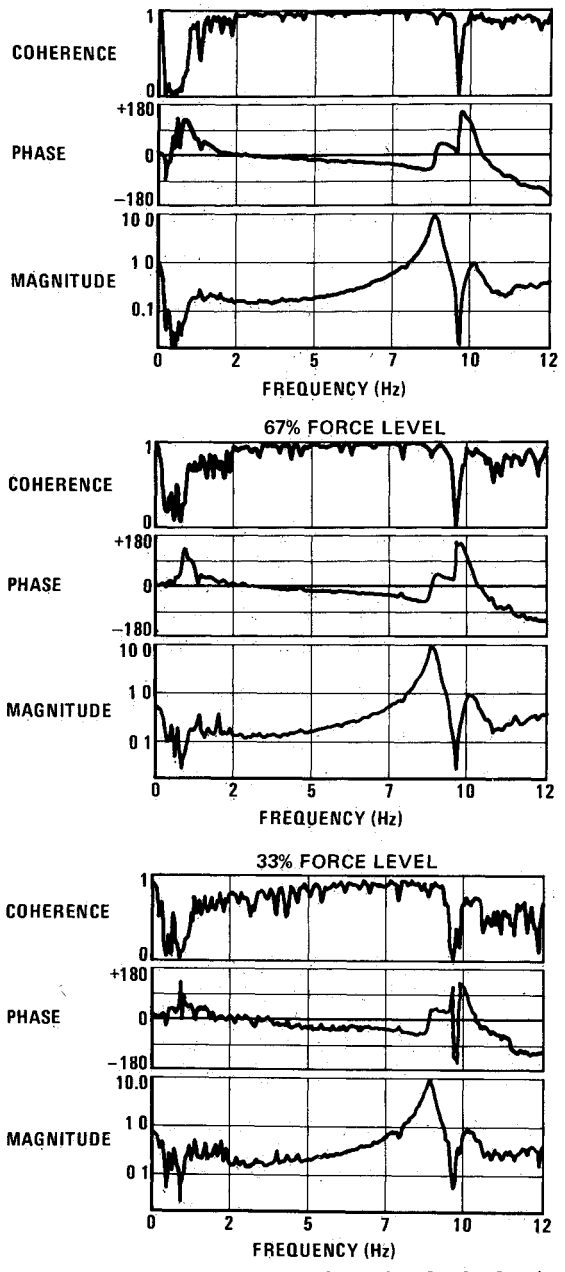

Fig 7 Open loop FRF measurements for various levels of excitation; $M=0\ 85$ $q=99$ psf, $\Delta f=0\ 04$, 32 averages

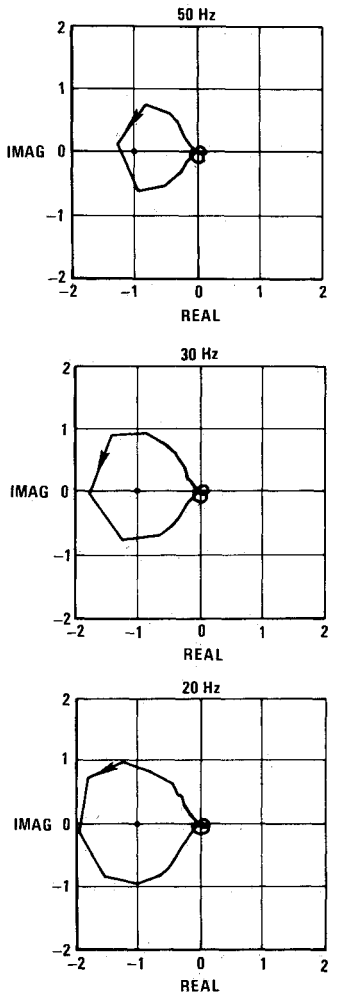

Fig 8 Open loop FRF measurements for various frequency resolutions; $M=0\ 85$, $q=99$ psf, 67% force, 32 averages

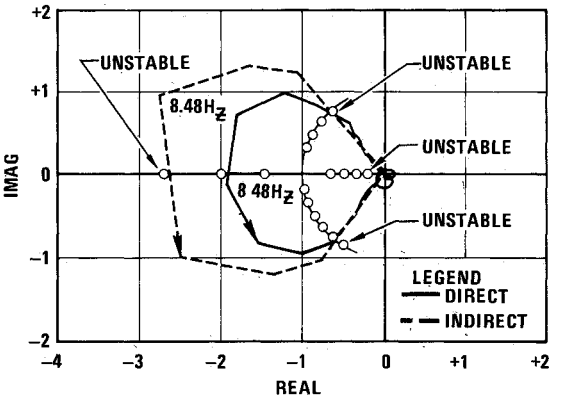

Fig 9 Control law gain and phase variation; $M=0\ 85$, $q=99$ psf, $\Delta f=0\ 04$ 32 averages

Open-Loop FRF Measurements

The effect of the magnitude of the excitation signal on the quality of the open loop FRF measured by the direct method is shown in Fig 7. The measurements were made at 99 psf dynamic pressure at a 0 85 Mach number which can be seen in Fig. 6 to be deep into the flutter region The upper limit of the spectral analyzer was set at 20 Hz ($\Delta f=0\ 04$ Hz) but the data are shown only up to 12 Hz to focus on quality of the data near the flutter frequency The 100% force level was the maximum excitation signal applied to the servoactuator that was considered safe That level produced an rms control surface commanded displacement of approximately 0 5 deg over a frequency range from 0 to 16 Hz It can be seen that the coherence function is only slightly degraded at the 67% force level but is considerably degraded at the 33% level The 67% level was used for most FRF measurements

The effect of frequency resolution on the accuracy of the open loop FRF measured by the direct method is shown in Fig 8 for the same Mach number and dynamic pressure point in Fig 7 The three plots show the effect of frequency resolution The upper plot was obtained with the upper limit of the frequency range set at approximately 50 Hz. Hence, the 512 points have a delta frequency of 0 10 Hz As the upper limit of the frequency is reduced to 30 and 20 Hz, the frequency increments became 0.06 and 0 04 Hz, respectively. A significant difference in the three plots is the magnitude of the upper crossover point which varies from approximately 1.25 to 1 8 to 2 0 as the frequency resolution is improved All three of these FRF were acquired with 32 averages obtained from records with a 75% overlap Hence the total data

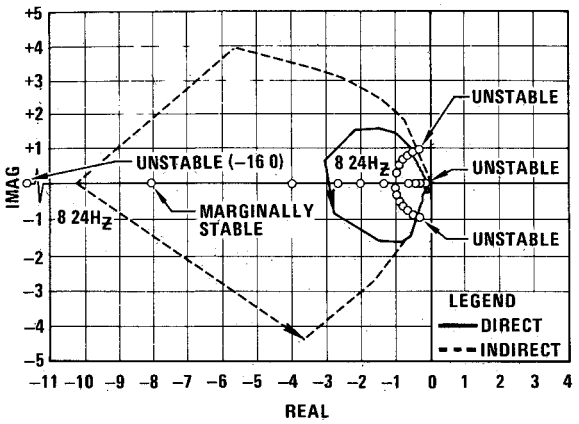

Fig 10 Control law gain and phase variations; $M = 0\ 85$, $q = 150$ psf $\Delta f = 0\ 04$ 32 averages

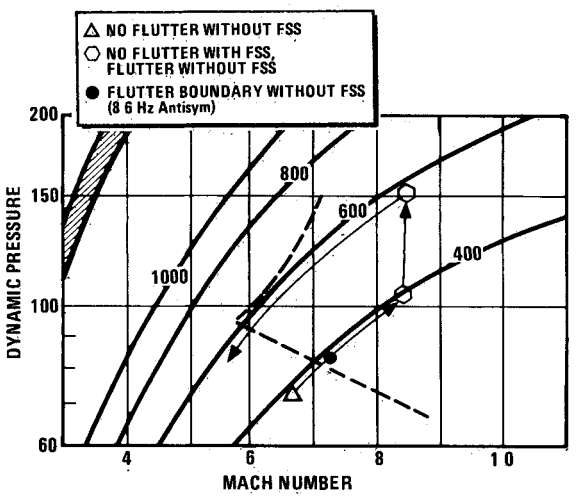

Fig 11 Test conditions for Configuration 33 single actuator tests

acquisition time varied from 88 s for the 50 Hz limit, to 146 s for the 30 Hz limit, and 219 s for the 20 Hz limit

To determine the accuracy of the measured open loop FRF, four points associated with the CCW loop were measured explicitly The FRF shown in Fig 8 with the 20-Hz frequency range is shown in Fig 9 as the solid line To determine the true upper crossover point, the gain in Eq. (1) was reduced incrementally until the model became unstable This was accomplished by implementing the FSS control law with both the in the loop (I) and the out of the loop (O) circuits The gain in the O circuit was reduced and switched with I The model then was checked visually to determine its stability. If the model was still stable the loops were switched back and the gain in the O circuit reduced further. This operation was repeated until the gain was reduced to the point that the model became unstable At that point the loops were again switched to return to the original gain The variation in gain is shown by the circular symbols on the negative real axis It is convenient to visualize each circle as a movement of the $(-1,0)$ point Hence, if the open-loop FRF measured by the direct method were accurate the model would have become unstable when the gain was reduced by a factor of 2 which can be visualized as moving the $(-1,0)$ point to the $(-2,0)$ point But the model did not go unstable until the gain was further reduced Hence the true upper crossover point is between $-2\ 0$ and $-2\ 7$ The gain was then increased until the model became unstable These points are also shown in Fig 9 and indicate that the true lower crossover point is only slightly higher than indicated by the measured open loop FRF The process was conducted also with the FSS nominal gain held constant and the phase shift of Eq. (1) varied in 10 deg increments It can be seen in Fig 9 that the phase margins measured in this manner compared very favorably to corresponding points in the measured open loop FRF Also superimposed in Fig 9 with dashed lines is the open loop FRF measured by the indirect method The indirect method predicts the upper crossover point much better

Figure 10 shows data that were obtained in the same manner as the data shown in Fig 9, except that they were obtained at a higher dynamic pressure It can be seen that the upper crossover point obtained from the open loop FRF as measured by the direct method and the upper crossover point obtained by reducing the gain differ to a larger extent in Fig 10 than in Fig 9 This larger difference is probably caused by the dynamic pressure at which the measurement was made being closer to the upper flutter boundary than the dynamic pressure of Fig 9 was to the lower flutter boundary However the open loop FRF as measured by the indirect method predicts the upper crossover point very well

Single Actuator Tests

Store Configuration 33 was tested also with one servoactuator The wind tunnel path over which the model was tested is shown in Fig 11 The model was first tested without the FSS engaged to the flutter condition indicated by the solid circular symbol Then the test conditions were reduced to the point indicated by the triangular symbol At that condition control law CL103 was implemented The open-loop FRF was measured with both actuators active to confirm that the control law had been implemented correctly Then one actuator was deactivated such that the flaperon which it normally actuated was locked in a neutral position The model was then tested along the wind tunnel path shown in Fig. 11 At the condition indicated by the hexagon at Mach number 0.85 and a dynamic pressure slightly above 100 psf the open loop FRF was measured The measurement indicated that the gain margin had been reduced by approximately a factor of 2 when compared with corresponding data measured with both actuators active However, the model was still stable Referring to Figs 9 and 10, it can be seen that the true gain margins measured with both actuators indicated that the model would be stable at both wind tunnel conditions with the gain reduced by a factor of 2 Hence, the same control law developed with both flaperons active was effective in suppressing flutter with a simulated failure of one actuator

Configuration 12

Configuration 12 has a full 370 gallon tank on the inboard station, nothing on the next outboard station, an AIM 9 on the next outboard station, and only the AIM-9 launcher on the tip station This configuration flutters in a symmetric mode at a frequency of 10.6 Hz. The analytically developed control law used sensor 2 and was identified as CL400. However, when the open loop FRF was measured with this control law at a wind tunnel condition below the flutter region, a large CW loop at 1 2 Hz appeared There did not appear to be any way to orient the 10 6 Hz loop in the desired position without locating the 1 2 Hz loop in a position that would cause a low frequency instability The open loop FRFs of the other sensors were examined and sensor 5 (Fig 4) was selected and a control law identified as CL406 was developed on line and is defined by

$$
\begin{array}{llll}
s/(s+20) & = \text{engaged} & G_2 & = G_3 = 0 \\
\omega_r & = 67 \text{ rad/s} & G_\Sigma & = 20\ 0 \\
G_1 & = -2\ 55 & \tau_1 & = 0 \\
\phi_1 & = 0\ 0 \text{ deg} & \tau_2 & = 0\ 15 \text{ s}
\end{array} \qquad (6)
$$

The flutter boundary without the FSS engaged is defined by the three solid circular symbols shown in Fig 12 With CL406

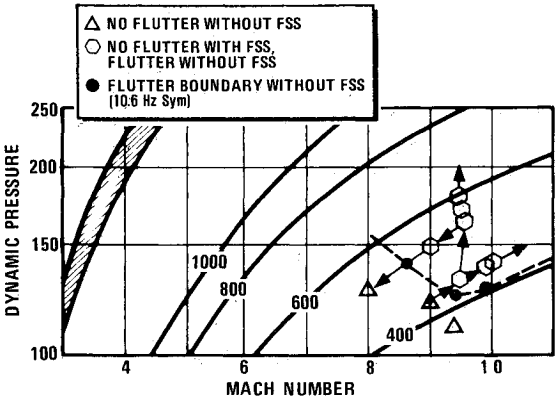

Fig 12 Test conditions for Configuration 12

engaged the model was tested in the flutter region as indicated in Fig 12 Again the FSS was disengaged temporarily to confirm that the model was in the flutter region

Conclusions

The uncertainty associated with the 1979 tests of Con figuration 33 was resolved Flutter regions were determined in an explicit manner by disengaging the FSS The accuracy of the measured open loop FRF was evaluated by determining the upper and lower gain margins and the positive and negative phase margins directly It was found that both the direct and indirect methods of measuring the open loop FRF predicted the phase margins and the lower crossover point very well The indirect method also predicted the upper crossover point very well, but the direct method predicted upper crossover points that were too low The accuracy was considerably improved by increasing the frequency resolution of the open loop FRF measurement A single actuator failure was demonstrated successfully The gain margin associated with the upper crossover point was reduced by approximately 50% by deactivating one actuator Both symmetric and antisymmetric flutter suppression were demonstrated

The technology for the design and application of nonadaptive FSS is sufficiently developed to warrant ap plication to either flight test demonstration aircraft or operational aircraft

Acknowledgment

This work was sponsored by the Air Force Wright Aeronautical Laboratories under Contract F33615 80 C-3210

References

[1] Peloubet R P Jr Haller, R L and Bolding R M F 16 Flutter Suppression System Investigation *Proceedings of the AIAA/ASME/SAE 21st Structures Structural Dynamics and Materials Conference* May 1980

[2] Peloubet R P Jr Haller R L and Bolding, R M. F 16 Flutter Suppression System Investigation Feasibility Study and Wind Tunnel Tests *Journal of Aircraft* Vol 19 Feb 1982 pp 169 175

[3] Peloubet R P Jr Haller R L and Bolding R M , F 16 Active Flutter Suppression Program, *Proceedings of the DGLR International Symposium* Nurnberg FRG Oct 1981

[4] Peloubet R P Jr and Haller R L , Wind Tunnel Demon stration of an Active Flutter Suppression System Using F 16 Model with Stores Vol I AFWAL TR-83 3046 April 1983

[5] Peloubet R P Jr. and Bolding R M , Summary of Active Flutter Suppression Research at General Dynamics Fort Worth Division AFWAL TR 83 3042 Jan 1983

[6] Hwang, C Johnson, E H , Joshi D S and Harvey C A Test Demonstration of Digital Adaptive Control of Wing/Store Flutter Part II: Adaptive Control ' AFWAL TR 82 3044 Dec 1982

[7] Newsom J R Abel I , and Dunn H J 'Application of Two Design Methods for Active Flutter Suppression and Wind Tunnel Test Results ' NASA TP 1653 May 1980

[8] Abel I Perry III B and Newsom J R ' Comparisons of Analytical and Wind Tunnel Results for Flutter and Gust Response of a Transport Wing with Active Controls, NASA TP 2010 June 1982

[9] Johnson E H Hwang C Pi W S Kesler D F , and Joshi D S ' Test Demonstration of Digital Control of Wing/Store Flutter *Proceedings of the AIAA/ASME/SAE 23rd Structures Structural Dynamics and Materials Conference* May 1982